Development of Stand-Alone Photovoltaic System Test-Bed using Neural Network based Solar PV Array Emulator

M.Ulaganathan* D.Devaraj R.Muniraj*****

* *Department of Electrical and Electronics Engineering, P.S.R. Engineering College, Sivakasi, Tamil Nadu, India-626140. (e-mail:ulagu.er@gmail.com).*
** *School of Electronics, Electrical and Biomedical Technology, Kalasalingam Academy of Research and Education,Srivilliputtur,Tamilnadu, India-626126 (e-mail:deva230@yahoo.com)*
*** *Department of Electrical and Electronics Engineering, P.S.R. Engineering College, Sivakasi, Tamil Nadu, India-626140. (e-mail: munirajphd@gmail.com).*

Abstract: Research on solar power generation is gaining momentum in recent decade, which requires a costly and complex experimental setup. The Photo-Voltaic (PV) source emulator is a necessary equipment to evaluate Maximum Power Point Tracking (MPPT) algorithm, power converters, and corresponding control algorithm. This paper proposes a novel Neural Network (NN)-based Solar Array Emulator (SAE) to emulate PV array characteristics. The reference model of the proposed SAE has been developed using NN, which can replicate a PV array characteristics with a programmable DC power source's support. A 640 W stand-alone PV array has been designed and tested using the proposed SAE to validate the performance of the developed prototype under different environmental conditions. The results demonstrate that the developed SAE has good accuracy in replicating the PV array characteristics than the conventional diode-based SAE.

Keywords: Neural Networks; Solar Array Emulator; Diode-based Solar Array Emulator; Programmable DC power source; Perturb and Observe (P&O) MPPT algorithm

1. INTRODUCTION

Solar Power Generation (SPG) is a promising alternative for fossil fuel-based power generation. The installation of the solar Photo-Voltaic (PV) array is quite essential to test and analyze SPG components. The PV array exhibits non-linear characteristics. Hence, repeatability during evaluation cannot be achieved under varying environmental conditions (Mai et al., 2017). 61683:1999 (E) standards recommend employing Solar Array Emulator (SAE) in analyzing and evaluating the performance of the SPG system (Cupertino et al., 2017),(Hunter et al., 2019),(Khan et al., 2019). SAE is a programmable DC source that mimics the PV array characteristics under controlled and uncontrolled environmental conditions (Ram et al., 2018).
A typical SAE includes a PV array reference model, reference tracking algorithm, and power stage. The PV array reference model mimics the electrical characterictics of the PV array characteristics Razman and Wei (2017a). The reference tracking algorithm of the SAE is responsible for monitoring the operating parameters of the SAE Razman and Wei (2017c). The SAE power stage plays a significant role in reproducing the emulated electrical characteristic produced by the PV array reference model into real electrical power Razman and Wei (2017a,c).
The SAE reference model is classified into i) Electrical equivalent model Restrepo et al. (2021) Tang et al. (2012) Ishaque et al. (2011) ii) PV parameters interpolation model Razman and Wei (2017c) Gonzalez-Llorente et al. (2016) Xenophontos et al. (2014) iii) Neural Network (NN)-based model Piazza et al. (2010)Razman and Wei (2017b). The electrical equivalent reference model of SAE uses Kirchhoff's circuit laws to derive the PV source characteristics equation Piazza and Vitale (2012). The single and double diode models with series, shunt resistance are the two electrical equivalent models of PV sources that are commonly discussed in the SAE literature Chin et al. (2015) Sampaio and Silva (2017)Hassan Hosseini and Keymanesh (2016). The estimation of internal parameters of these models is done using optimization techniques like genetic algorithm Zagrouba et al. (2010) Ulaganathan and Devaraj (2016) and differential evolution technique Muhsen et al. (2015). These optimization techniques estimate the internal parameters by measuring the PV sources operating parameters at Maximum Power Point (MPP). Even though these techniques are simple, the operating point inaccurate measurement significantly affects the PV model accuracy. The interpolation-based SAE reference model is a mathematical function that reproduces the PV model's characteristics curve using the operating parameters like Open-Circuit Voltage (V_{OC}) and Short-Circuit Current

(I_{SC}) Khouzam and Hoffman (1996) Kim et al. (2013). Generally, the PV module manufacturer provides the value of V_{OC} and I_{SC} at Standard Test Condition (STC) only, which reduces the adaptability of the SAE reference model at various operating conditions.

A few authors have used the NN-based PV sources reference model for SAE. In the NN-based SAE reference model, Current-Voltage (I-V) characteristics dataset is collected in real-time. The collected dataset is utilized for training the NN-based reference model. The trained NN model estimates the operating parameters of the PV array and is incorporated in the SAE. The Growing Neural Gas (GNG) network used in developing the NN-based reference model is discussed in Piazza et al. (2010). The GNG network permits the growth of the number of hidden neurons to meet the goal with lesser computational difficulties. In Razman and Wei (2017b), the NN-based adaptive controller has been proposed to improve the SAE reference model dynamic performance.

The reference tracking algorithm tracks the operating voltage and current of SAE. It compares it with the I-V characteristics curve generated by the SAE reference model to the resistance connected at the output side of SAE. Frequently-used reference tracking algorithms are direct referencing Di Piazza et al. (2010) Ayop et al. (2018) Ayop and Tan (2018) and resistance comparison Ayop and Tan (2018) methods. The direct referencing method is an iterative technique that determines the SAE operating points either using voltage or current input. The resistance comparison algorithm uses resistance as input and tracks the SAE output voltage and current. A resistance comparison algorithm and PI controller implemented in buck converter-based SAE are discussed in Razman and Wei (2017b) Ayop and Tan (2018). This approach increases the implementation difficulties and affects the stability and flexibility under changing load and environmental conditions.

Programmable DC power supplies and DC-DC converters are the generally preferred power stage for SAE development. The buck converter-based SAE discussed in Ayop and Tan (2018) Azharuddin et al. (2016) requires a reference tracking algorithm along the adaptive controller to improve the dynamic response. In addition, large LC filters need to be fixed to minimize the SAE voltage and current ripples.Implementing a complex reference tracking algorithm requires a digital controller Moussa and Khedher (2019) Moussa et al. (2019), which works with extensive sampling time, which leads to the incorrect control response, which greatly affects the stability and accuracy of the converter based-SAE. DC programmable power supply based-SAE has been discussed in Mukerjee and Dasgupta (2007) Abbes et al. (2014) Ulaganathan and Devaraj (2019) . The power supply-based SAE works on simple analog controllers and resistance comparison-based reference tracking algorithm. Hence, power supply-based SAE has better repeatability with improved output stability and reduced complexity during hardware implementation.

A novel Neural Network-based SAE has been proposed in this paper. The NN has been adopted to develop the reference model of the proposed SAE. The experimental data collected from the real PV array have been utilized to develop the NN model. The reference model of the SAE is developed in the MATLAB environment and implemented in the LabVIEW control and simulation loop to emulate the PV array characteristics. The developed NN-based reference model does not require operating parameter details and precise measurement of the particular operating points on the characteristics curves. Therefore, it improves the accuracy and flexibility of the SAE. The proposed NN-based SAE adopts online load tracking as a reference tracking algorithm. The developed reference tracking algorithm is a straightforward technique. It does not require an additional control loop to monitor the output voltage and current of the SAE, which enhances the stability and dynamic response of the SAE. The Programmable DC power source is the proposed SAE power stage, replicating the PV array characteristics with analog controller support. The developed SAE has an NN-based reference model and an online load tracking algorithm implemented in the analog controller to control the SAE power stage, reducing computational and hardware implementation difficulties. Further, the developed NN-based SAE can emulate both static and dynamic characteristics of the PV array. Hence, the developed NN-based SAE is more suitable for emulating the PV array.

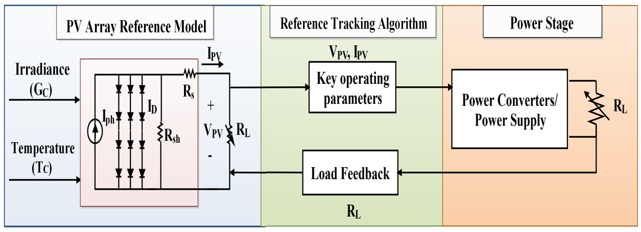

Fig. 1. The major components of Solar Array Emulator

2. DESCRIPTION OF THE PROPOSED NEURAL NETWORK-BASED SOLAR ARRAY EMULATOR

Fig.1 depicts the three components of an SAE, namely the PV source reference model, reference tracking algorithm, and power stage.The SAE reference model decides the SAE's accuracy; therefore, the reference model must be precise and straightforward without sacrificing the correctness of the PV array characteristics. The reference tracking algorithm connects the reference model and power stage for the smooth operation of SAE. Hence, the reference tracking algorithm should be stable, have less computational complexity, easy to implement, and be adaptable to varying operating conditions. The power stage of the SAE has to mimic the reference model dynamics with minimum output deviation in a short time. Therefore, the SAE power stage should work with an adaptable reference tracking algorithm implemented in the analog controller.

The schematic diagram of the NN-based Solar PV Array Emulator is depicted in Fig.2 The proposed system adopts the data-driven modeling approach for the SAE reference model development, which learns the PV array model from the input and output dataset. The proposed SAE uses an NN-based reference model, which estimates the optimum PV array Voltage $V_{PV(Est)}$ and Current $I_{PV(Est)}$ parameters are estimated using Feed Forward Neural Network. Data collected under various environmental and loading conditions from a real PV array are used to develop the NN-based reference model of the proposed SAE. The NN model inputs are irradiation, temperature, and load, which in turn estimate the PV array Voltage $V_{PV(Est)}$ and Current $I_{PV(Est)}$ accurately. The proposed SAE integrates the reference model into a programmable DC power supply through an online load tracking based on the Co-simulation technique. The proposed reference tracking algorithm utilizes the NN estimated operating parameters of the SAE as the control signal and load connected to the SAE as the feedback signal. The NN model outputs are converted into analog signals, namely $V_{PV(Est)}$' and $I_{PV(Est)}$'. These values are used as the control signal to reproduce the SAE reference model's dynamics using the SAE power stage. The SAE power stage receives the $V_{PV(Est)}$' and $I_{PV(Est)}$' through the analog controller platform called National Instrument (NI)-myDAQ and generates linearized emulated operating points of NN-based SAE namely voltage (V_{PV}) and current (I_{PV}) proportional to it. These mimicked operating values were measured across the load feedback into the NN model to track SAE operation using the online load tracking algorithm. The proposed SAE is developed in three stages.

(a) Reference model development using Artificial Neural Network.
(b) Online Load Tracking Integration.
(c) Monitoring and Control of Programmable DC power supply.

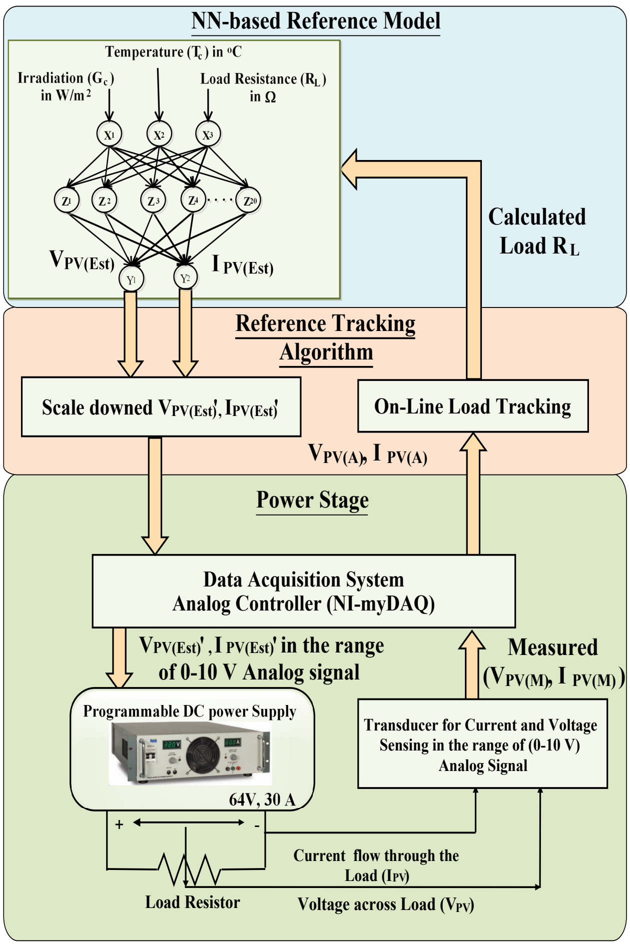

Fig. 2. Schematic diagram of the Proposed NN-based SAE

3. REFERENCE MODEL DEVELOPMENT USING ARTIFICIAL NEURAL NETWORK

Artificial Neural Network (ANN) is a technique influenced by brain functioning and its decision-making mechanism. It consists of a large number of neurons connected to process information. The interconnection and arrangement of neurons define as the architecture of ANN. Multi-Layer Feed Forward (MLFF) Neural Network Sivaneasan et al. (2017) Yaïci et al. (2017) is used in this work for estimating the $V_{PV(Est)}$ and $I_{PV(Est)}$ of the PV array. A typical MLFF neural network is a cascaded layer of the neurons (namely input, hidden, and output layer), transferring information in the forward direction. A single neuron's expression in the network is the sum of all its weighted inputs passing through a non-linear activation function Samara and Natsheh (2018) Shuvho et al. (2019).The hidden layer neuron output and its sigmoid activation function are mathematically expressed by Equation (1) and Equation (2)

$$net_h = \sum_{i=0}^{n} x_i^k . w_{hi}^k + b_i \tag{1}$$

$$Z_h = f(net_h) \Longrightarrow \frac{1}{1 + e^{-\eta . net_h}} \tag{2}$$

Where 'i' and 'h' denotes input and hidden layer neurons respectively. Z_h represents the output of the h^{th} hidden layer neuron. xi is the output of ith input layer neuron. The connection weight between the h^{th} neuron and the i^{th} neuron is denoted as 'w_{hi}'. bi is the bias constant and η is the activation gain of sigmoid function.

3.1 Estimation of Optimum operating parameters of PV array using Neural Network

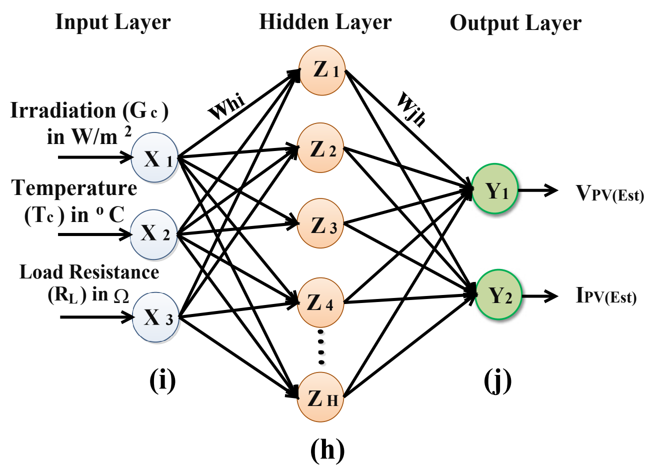

Fig. 3. Multilayer Feed-Forward Network for estimating PV array output Voltage $V_{PV(Est)}$ and Current $I_{PV(Est)}$

Fig.3 shows the proposed MLFF NN structure for estimating the PV array $V_{PV(Est)}$ and $I_{PV(Est)}$. The MLFF NN has development and operational stage. TThe NN model development is carried out using real-time experimental data collected from a PV array. The collected data is separated into training data and test data. Training data is utilized to develop the network, and test data

is used to evaluate the developed network's performance. The network is trained using the training data set during the development stage, consisting of input variables and corresponding output variables samples. During training, the MLFF makes use of the connecting weight to map the relationship between the input variables (irradiation, temperature, and loading conditions) and the output variables ($V_{PV(Est)}$ and $I_{PV(Est)}$).
During training, irradiation data's bigger value may suppress the smaller value of temperature and load data. Apart from this, when raw data is applied to the network, it may tend to saturate the neurons. This saturated neuron produces no output value changes, even for more significant changes in the input value. Hence, the raw data is normalized using (3) to avoid the above issues.

$$y_n = \frac{(y - y_{\min}) \times range}{(y_{\max} + y_{\min})} + staring\ value \tag{3}$$

Where y_n - Normalized value; y_{max} and y_{min} -Maximum and Minimum values of the variables 'y'.
To train the network, initially, random values are assigned to all the weights in the network. Then the training algorithm is applied to adjust the weights. The learning algorithm used to train the MLFF NN is called the backpropagation algorithm. The algorithm performs feed-forward propagation of input, error backpropagation, and weights updating or adjustment. The input data goes through the hidden layer and arrives at the output layer. The output of the network is given by a summation function expressed by (4).

$$y_j^k = f(net_j^k) \Longrightarrow f\left[\sum_{j=1}^{n} w_{jh}^k z_h^k + b_j\right] \tag{4}$$

The effectiveness of the training process is evaluated using the performance indices. The performance index used in this work is Mean Square Error (MSE), which acts as the learning goal, which is given by (5).

Error Function:

$$E^k = \frac{1}{2}\sum_{j=1}^{m}(d_j - y_j^k)^2 \tag{5}$$

Where 'j' and 'h' denote the indices of output and hidden layer neurons, respectively. 'z_h^k', represents the output of the 'z^{th}' hidden layer neuron. 'm' and 'n' represent the number of input and output variables. 'w_{jh}' denotes the connection weight between the 'h^{th}' neuron and the 'j^{th}' neuron. 'b_j' and 'k' represent the bias constant and iterations. . 'd_j' and 'y_j^k' represent the desired and actual output of the j^{th} output layer neuron.The weight adjustment process is continued during the training process until it reaches the set learning goal.
The weight adjustment equations are given as Input to Hidden Layer neurons:

$$w_{hi}^{k+1} = w_{hi}^k + \eta\delta_h^k.x_i \tag{6}$$

Hidden to Output Layer neurons:

$$w_{jh}^{k+1} = w_{jh}^k + \eta\delta_j^k.Z_h \tag{7}$$

Where η - Learning rate; δ_h^k- Deviation of hidden layer; δ_j^k- Deviation of hidden layer;
Once the training is over, the estimation performance evaluation of the developed network is done using the test data. The trained network holds the updated weights, which provides a solution to meet the expected output. The developed NN model's testing is done with the testing data set, following the training stage. Once the developed network's training and testing are completed, it is ready to estimate the $V_{PV(Est)}$ and $I_{PV(Est)}$ for the unknown inputs.

4. ONLINE LOAD TRACKING ALGORITHM INTEGRATION

The developed online load tracking algorithm calculates the load connected to the SAE power stage and feeds back the same to the reference model of NN-based SAE. The V_{PV} and I_{PV} output of the SAE is measured across the load resistance connected to the SAE power stage. These measured values are scaled downed into $V_{PV(M)}$ and $I_{PV(M)}$ with a voltage transducer in the range of 0 - 10 V and acquired using the NI-myDAQ. The acquired $V_{PV(M)}$ and $I_{PV(M)}$ are collected in the LabVIEW and up-scaled into the actual measured PV array voltage $V_{PV(A)}$ and current $I_{PV(A)}$. The online load tracking algorithm monitors $V_{PV(A)}$ and $I_{PV(A)}$ and computes load resistance ($R_L = V_{PV(A)} / I_{PV(A)}$) online. During the initial iteration, the resistive load is fixed to the maximum under constant irradiation and temperature. Under this condition, the reference model estimates the output voltage $V_{PV(Est)}$ and output current $I_{PV(Est)}$ of the PV array, which is mimicked by the SAE power stage.
The SAE power stage voltage output V_{PV} is measured across the load that equals the emulated PV array V_{OC}. The load resistance value is adjusted, the DC power supply generates different values of V_{PV}, and the corresponding I_{PV} values are measured in series with the load resistance. Subsequently, the LabVIEW control and simulation loop computes the updated load resistance R_L value and feeds it back into the reference model of NN-based SAE. With the decrease in resistor value, V_{PV} value also decreases, and I_{PV} value increases consequently. When the resistor value is adjusted to a minimum, the I_{PV} value reaches the emulated PV array I_{SC}. Under different environmental conditions, the emulated PV array characteristics have been obtained by repeating the above-said procedure by changing the irradiation and temperature values in the NN-based SAE. Fig.4 depicts the flowchart of the online tracking algorithm integration. The proposed SAE is developed without iterative loops and sophisticated control loops to emulate the PV array, as implemented Mai et al. (2017) Mukerjee and Dasgupta (2007).

5. MONITORING AND CONTROL OF PROGRAMMABLE DC POWER SUPPLY

The estimates value $V_{PV(Est)}$, and $I_{PV(Est)}$ of the reference model are scaled-down as $V_{PV(Est)}$' and $I_{PV(Est)}$' in the reference tracking algorithm stage. These scaled-down values are used to drive the SAE-power supply through the National Instrument (NI)-myDAQ, which acts as a control signal in the power stage. Subsequently, the SAE-power supply generates the V_{PV} and I_{PV} outputs of the SAE. Online load tracking is integrated with the programmable DC power supply to monitor the SAE output's correctness in the reference tracking stage. The online load tracking monitors the SAE operations and generates the feedback signal to the SAE reference model.

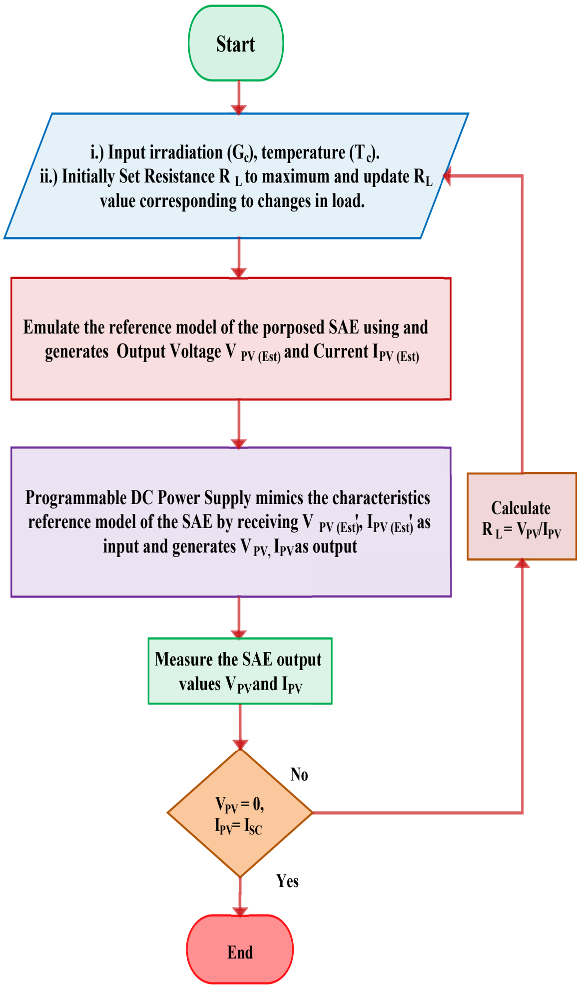

Fig. 4. Flow chart describing the working of the online tracking algorithm

6. RESULTS AND DISCUSSION

This section presents the steps involved in developing the reference model, reference tracking algorithm of the SAE, and experimentation conducted using the developed SAE. The proposed SAE is designed to emulate a 640 W PV array and steady-state characteristics analysis is done at STC. The relative error and emulation efficiency is calculated between operating parameters of the theoretical and emulated PV array. The experimental results are compared with the diode-based SAE to demostrate the correctness of the proposed NN-based SAE.

6.1 Development of Reference model for NN-based SAE

In the present work, NN is used for the development of the SAE reference model. For the NN-based reference model development, experimental data is collected from an actual PV array with a peak power of 640 W. The PV array consists of 8 PV modules connected in the array size of 2×4. The key operating parameters of the Sukam PV module are given in Table-1.

The PV array and data logging unit used to collect the data is shown in Fig.5. The PV array is directly connected with the 50 Ω rheostat (load), and output voltage (V_{PV})

Table 1. Electrical parameters of the Sukam PV module

Specifications	**Value**
Voltage at P_{MPP} (V_{MPP})	17.4 V
Current at P_{MPP} (I_{MPP})	4.6 A
Maximum Power Point (P_{MPP})	80.04 W
Short-Circuit Current (I_{SC})	5.2 A
Open-Circuit Voltage (V_{OC})	21.2 V

and current (I_{PV}) values are measured under different environmental and loading conditions. Davis make irradiation sensor is used in this study, which can measure irradiation level of $0 - 1.6$ kW/m^2 and gives a voltage output of $0 - 1.6$ V. The load is varied by adjusting the load resistance between 0 Ω – 50 Ω. The temperature sensor used in the system can measure up to 100 °C and scales the measured temperature data to $0 - 5$ V. The irradiation and temperature sensor outputs are collected through NI myDAQ. The PV array voltage and current values are measured using the voltage transducer and DC Shunt resistor in the data logging unit. The measured voltage and current values are also collected using NI myDAQ. The PV array's experimental data are collected from the installed location, which has a solar irradiation level ranging between 300 W/m^2 – 1200 W/m^2 and temperature level ranging between 28 °C–39 °C.Totally 3440 datasets of irradiation, temperature level, and load conditions along with the PV array output Voltage (V_{PV} and Current (I_{PV}) were collected. Out of the collected data set, 2408 datasets are used for training and the remaining data for testing. The developed Neural Network consists of three layers with one hidden layer. Irradiation, temperature, and load conditions are the NN input , and PV array output voltage and current are the output. The number of hidden layer neurons is selected on a trial and error basis. Tangent hyperbolic and linear activation functions are used in the hidden layer and output layer neurons.

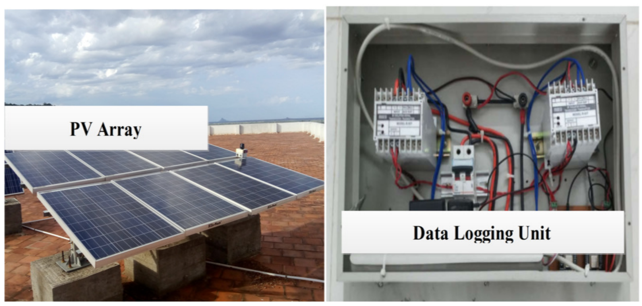

Fig. 5. Solar PV array and its data logging unit

The Levenberg-Marquardt algorithm is used to train the network until it meets the Mean Square Error (MSE) of 1.9×10^{-3}. The Neural network is developed using MATLAB neural networks toolbox. The developed NN exhibited satisfactory performance with 20 hidden layer neurons and reached the error goal in 3678 epochs with the testing Root Mean Square Error (RMSE) of 0.0139, illustrated in Fig.6 and Fig.7. After successfully training the network, about 1032 datasets were used to test the trained network performance. The network took 437 ms to complete the testing with the testing MSE of 0.0127. The developed reference model of the proposed SAE can

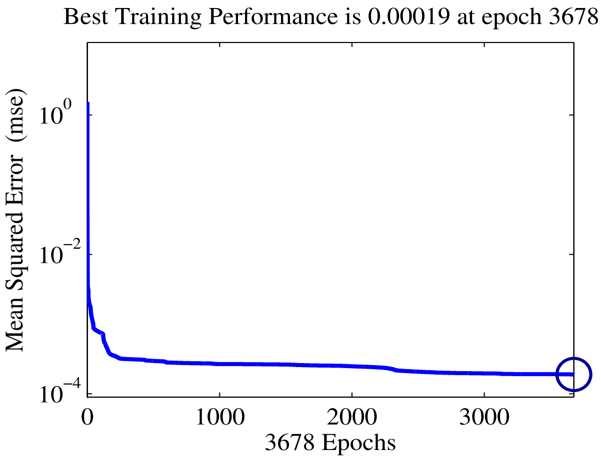

Fig. 6. Neural Network Training output performance.

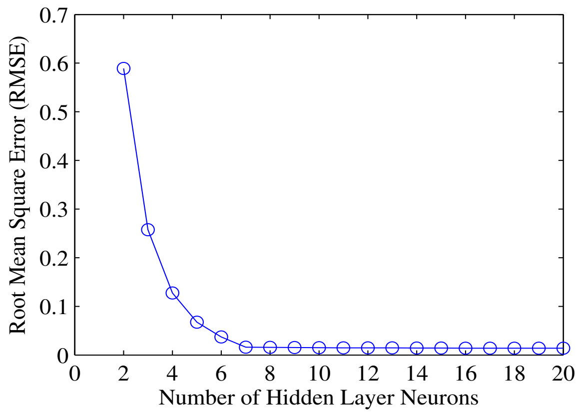

Fig. 7. RMSE vs Number of Hidden Layer Neurons.

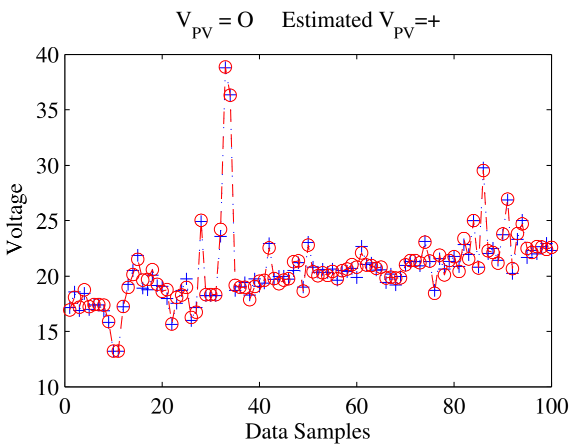

Fig. 8. Estimated PV array Voltage $V_{PV(Est)}$.

estimate the $V_{PV(Est)}$ and $I_{PV(Est)}$ satisfactorily on completing the training and testing phase, which is depicted in Fig.8 and Fig.9. The developed neural network output matches the estimated output $V_{PV(Est)}$ and $I_{PV(Est)}$ values of the SAE reference model with measured V_{PV} and I_{PV} output of the PV array.

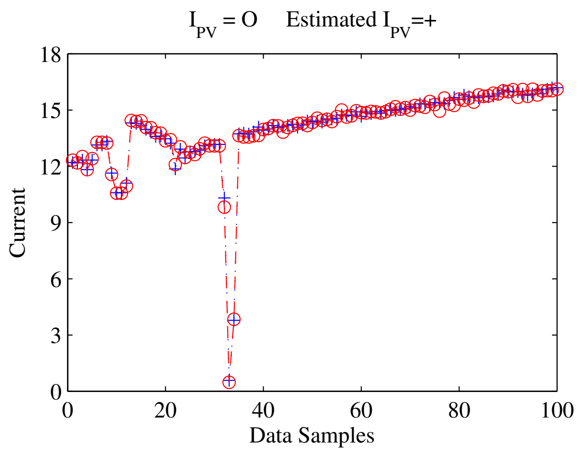

Fig. 9. Estimated PV array Current $I_{PV(Est)}$.

6.2 Performance Evaluation of the developed Reference model

A PV array with 640 W peak power output is used for carrying out the study . As discussed in the previous section, the reference model of NN-based SAE is trained and tested in MATLAB. The trained reference model of NN-based SAE is implemented in LabVIEW using the MATLAB script. The trained network is invoked inside the MATLAB script by initializing the "reference model" neural network file. The developed reference model in the MATLAB script receives input from LaBVIEW and estimates the emulated PV array voltage $V_{PV(Est)}$ and current $I_{PV(Est)}$. The simulation block of the developed NN-based reference model is shown in Fig.10. LabVIEW co-simulates the reference model in the control and simulation loop using Runga-Kutta-1 resolver with a step size of 1 millisecond. This developed SAE is simulated under STC, at which irradiation is 1000 W/m^2 and temperature is 25 °C. Fig.11 and Fig.12 show the P-V and I-V characteristic curves, respectively, of the simulated NN-based SAE.
The relative error is calculated to determine the accuracy of the reference model of NN-based SAE. Under STC, the relative errors of the PV array reference model are estimated using (8), and the results are tabulated in Table-2.

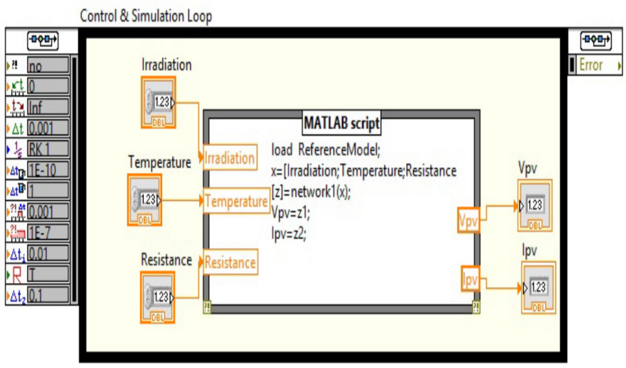

Fig. 10. Reference model simulation block of NN-based SAE

$$RelativeError(X) = \frac{|X_{\text{Theoretical}} - X_{\text{Simulated}}|}{X_{\text{Theoretical}}} \times 100\% \quad (8)$$

Where "X" is V_{OC}, I_{SC}, V_{MPP}, I_{MPP}, and P_{MPP}

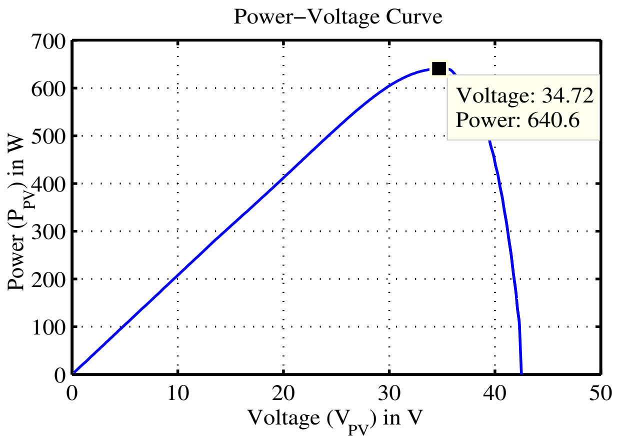

Fig. 11. P-V characteristics of the simulated NN-based SAE at STC .

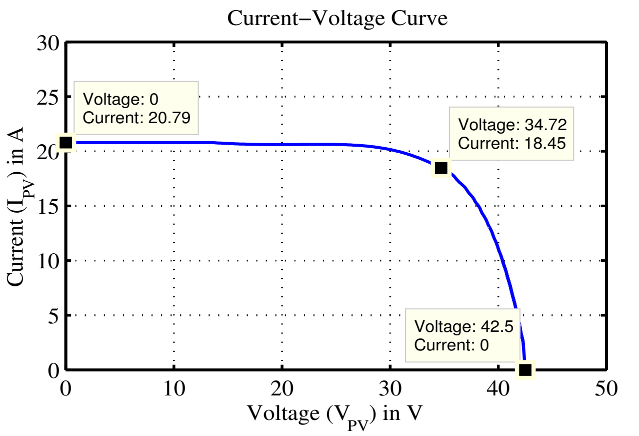

Fig. 12. I-V characteristics of the simulated NN-based SAE at STC .

Table 2. Relative error between the theoretical output and simulated output reference model output of PV array at G = 1000 W/m^{2}and T=25 °C.

Parameter	**Theoretical Output**	**Simulated Output**	**Relative Error %**
Open Circuit Voltage (V_{OC}) in V	42.4	42.49	0.21
Short Circuit Current (I_{SC}) in A	20.8	20.79	0.04
Voltage at P_{MPP} (V_{MPP}) in V	34.8	34.72	0.22
Current at PMPP (I_{MPP}) in A	18.4	18.45	0.27
Power at P_{MPP} in W	640.32	640.58	0.03

The Relative Error (RE) at Maximum Power Point (MPP) is 0.03 %, demonstrating the accuracy of the NN-based reference model. Thus, the developed reference model of PV array can be used for real-time emulation.

6.3 Hardware implementation of reference tracking algorithm of the proposed SAE

The hardware setup of the proposed SAE is shown Fig.13. The developed reference model of SAE has the maximum voltage $V_{PV(EST)}$ range of 0 – 42.49 V and the current $I_{PV(EST)}$ range of 0 – 20.79 A. The hardware setup is monitored and tracked with NI-myDAQ, which operates in the range of 0 – 10 V. Therefore, the $V_{PV(Est)}$ and $I_{PV(Est)}$ outputs of the NN-based SAE have to be scaled down to the range of 0 – 10 V using the (9) and (10).

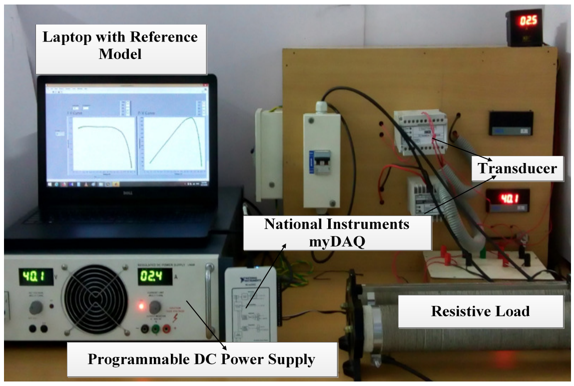

Fig. 13. The test setup of the proposed SAE

$$V_{\text{PV(Est)}}{}' = \frac{V_{\text{PV(Est)}}}{64} \times 10(V) \quad (9)$$

$$I_{\text{PV(Est)}}{}' = \frac{I_{\text{PV(Est)}}}{30} \times 10(V) \quad (10)$$

The calculated $V_{PV(Est)}$' and $I_{PV(Est)}$' are ported out at the NI myDAQ analog output port-1 and port-2 to regulate the SAE power stage. The Programmable DC power is chosen as the power stage in this work, which has a voltage range of 60 V and a maximum current rating of 25 A. The power stage is controlled using the programming voltage in the range of 0 –10 V. The SAE power stage output is measured across the resistive load using transducer and shunt resistance. The voltage transducer used for measuring voltage $V_{PV(M)}$ converts 0 –100 V into 0 –10 V. Similarly, for measuring current $I_{PV(M)}$, a DC shunt is used, measuring 0 – 50 A in terms of 0 – 75 mV. The measured current value is converted into 0 – 10 V using a voltage transducer. These measured $V_{PV(M)}$ and $I_{PV(M)}$ values are in the range of 0–10 V and fed back into the LabVIEW through NI-myDAQ, an analog input port -1 and port-2. These measured $V_{PV(M)}$ and $I_{PV(M)}$ values are scaled backed to the actual voltage $V_{PV(A)}$ and current $I_{PV(A)}$ values of the emulated PV array using (11) and (12) in the LabVIEW environment.

$$V_{\text{PV(A)}} = \frac{V_{\text{PV(M)}}}{10} \times 100(V) \quad (11)$$

$$I_{\text{PV(A)}} = \frac{I_{\text{PV(M)}}}{10} \times 50(A) \quad (12)$$

These calculated $V_{PV(A)}$ and $I_{PV(A)}$ are utilized to estimate the load resistance (R_L) in the online load algorithm.

The calculated R_L is given as input in the reference model developed in MATLAB script through LabVIEW.

6.4 Steady-State analysis under Standard Test Condition

To analyze the steady-state performance, the developed SAE is tested under constant irradiation and temperature level of 1000 W/m^2 and temperature is 25 °C are maintained throughout the test to acquire the PV source electrical characteristics. Therefore, the NN-based SAE is studied under STC to obtain their characteristics curves. For comparison, under STC, the characteristics curve is obtained using diode-based SAE also. Fig.14 and Fig.15 shows the P-V and I-V characteristics of NN-based SAE and diode-based SAE, which are experimentally obtained in real-time. Both the SAE reproduce the PV array characteristics with a small error around the key operating parameters of the PV array.

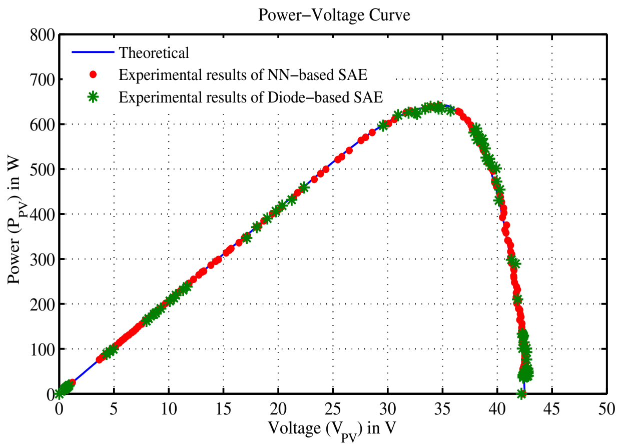

Fig. 14. P-V Characteristics curve of the theoretical and emulated PV array at Irradiation 1000 W/m^{2}and temperature is 25 °C .

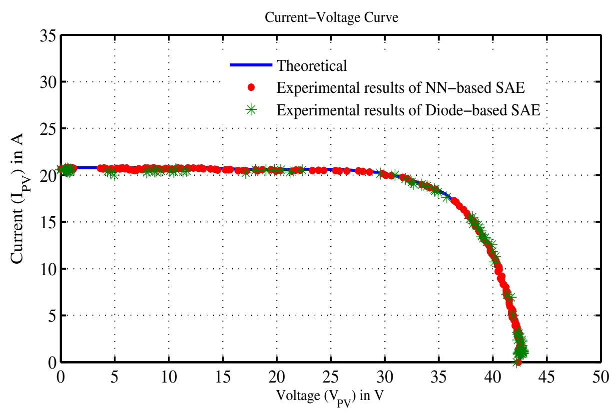

Fig. 15. I-V Characteristics curve of the theoretical and emulated PV array at Irradiation 1000 W/m^{2}and temperature is 25 °C .

The relative error is estimated between the key operating parameters of emulated and theoretical PV array using (8) to demonstrate the developed SAE's accuracy. The theortical PV array key opeating parameters are determined

Table 3. NN-based SAE relative errors at key operating parameters at G = 1000 W/m^{2}and T=25 °C.

Parameter	**Theoretical Output of PV array**	**NN-based SAE Emulated output**	
		Measured	**RE %**
Open-Circuit Voltage (V_{OC}) in V	42.4	42.54	0.24
Short-Circuit Current (I_{SC}) in A	20.8	20.69	0.53
Voltage at MPP (V_{MPP}) in V	34.8	34.7	0.29
Current at MPP (I_{MPP}) in A	18.4	18.49	0.49
Power at MPP (P_{MPP}) in W	640.32	641.6	0.20

Table 4. Diode-based SAE relative errors at key operating parameters at G = 1000 W/m^{2}and T=25 °C.

Parameter	**Theoretical Output of PV array**	**Diode-based Emulated output**	
		Measured	**RE %**
Open-Circuit Voltage (V_{OC}) in V	42.4	42.2	0.47
Short-Circuit Current (I_{SC}) in A	20.8	20.64	0.77
Voltage at MPP (V_{MPP}) in V	34.8	34.58	0.63
Current at MPP (I_{MPP}) in A	18.4	18.46	0.32
Power at MPP (P_{MPP}) in W	640.32	638.34	0.30

through the PV module flash test. The relative errors emulated PV array developed in NN-based SAE and diode-based SAE are calculated, and the results are presented in Table-3 and Table-4 respectively. The relative error of the maximum power point generated by the NN-based SAE is 0.2 %, which is less than the relative error of diode-based SAE.

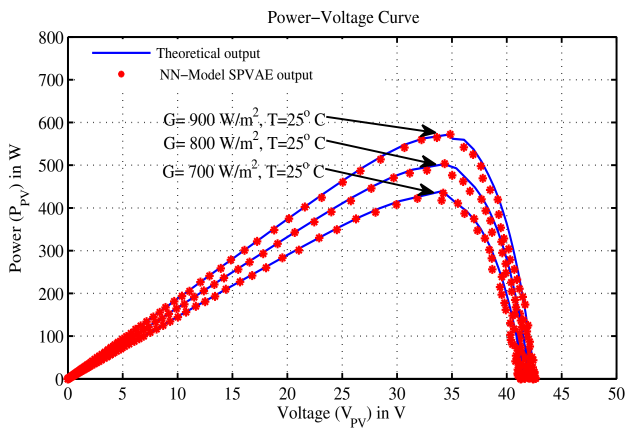

Fig. 16. Comparison of between the theoretical and emulated P-V characteristics curve of the PV array using NN-model-based SPVAE under different irradiation levels and constant temperature.

In addition, the NN-based SAE is tested under different environmental conditions to ensure their robustness. The emulation efficiency is calculated between theoretical (P_{MPP})(T) and emulated (P_{MPP})(E) PV array power output at MPP under different environmental conditions. The Fig.16 depicts the comparison results under different environmental conditions; emulation efficiency is tabulated in the Table-5.

Table 5. Emulation efficiency of the developed NN-based SAE under different environment conditions.

Irradiation Level in W/m^2	P_{MPP}(T) in W	P_{MPP}(E) in W	Emulation Efficiency in η%
900	572	571	99.83
800	502.53	501.2	99.71
700	440.12	434.4	98.7

The emulation efficiencies of the developed NN-SAE at 900 W/m^2 and 700 W/m^2 are 99.83 % and 98.7 % respectively, which is comparably improved with the emulation efficiency of diode-model SAE proposed by Nazar Ali et al. (2021).The relative error results of various parameters show that the developed reference model of NN-based SAE is comparable to the diode-based SAE reference model.The results demonstrate that the developed NN-based SAE has good accuracy in replicating the PV array characteristics in comparison with the Diode-model based SAE.

7. CONCLUSION

A novel neural network-based SAE using a programmable DC source is proposed in this work. The developed SAE prototype's performance has been tested under steady-state conditions. The relative error at emulated PV array power output at MPP is 0.2 %, which is less than the relative error of diode-based SAE. Further, the NN-based SAE emulation efficiency is improved than the diode-based SAE due to the precisely developed NN-based SAE reference model. Hence, the developed NN-based SAE is more suitable for emulating the PV array and to test the Maximum Power Point Tracking controllers, power converters used in the solar PV system.

The primary disadvantage of using a diode-based SAE is that it necessitates knowledge of the PV module specifications to accurately emulate the I-V characteristics of the entire PV array. This diode-model-based approach is suitable for small PV arrays with a capacity of less than 1 kW due to the computational burden of iterating the PV source characteristics equations. In contrast, the developed NN-based SAE approach can utilize real-time data gathered directly from the PV array without prior knowledge of PV source specifications. Therefore, NN-based SAE approach is better suited for emulating larger PV arrays with a capacity of over 1 kW. But,the developed NN-based SAE requires high-quality training data for reasonable accuracy. However, obtaining sufficient real-time data from the PV sources may be challenging and expensive sometimes, limiting the NN-based SAE's effectiveness.

REFERENCES

Abbes, D., Martinez, A., Champenois, G., and Robyns, B. (2014). Real time supervision for a hybrid renewable power system emulator. *Simulation Modelling Practice and Theory*, 42, 53–72.

Ayop, R. and Tan, C.W. (2018). Rapid prototyping of photovoltaic emulator using buck converter based on fast convergence resistance feedback method. *IEEE Transactions on Power Electronics*, 34(9), 8715–8723.

Ayop, R., Tan, C.W., and Lim, C.S. (2018). The resistance comparison method using integral controller for photovoltaic emulator. *International Journal of Power Electronics and Drive Systems*, 9(2), 820.

Azharuddin, M., Babu, T.S., Bilakanti, N., and Rajasekar, N. (2016). A nearly accurate solar photovoltaic emulator using a dspace controller for real-time control. *Electric Power Components and Systems*, 44(7), 774–782.

Chin, V.J., Salam, Z., and Ishaque, K. (2015). Cell modelling and model parameters estimation techniques for photovoltaic simulator application: A review. *Appl. Energy*, 154, 500–519.

Cupertino, A.F., Pereira, H.A., and Mendes, V.F. (2017). Modeling, Design and Control of a Solar Array Simulator Based on Two-Stage Converters. *J. Control. Autom. Electr. Syst.*, 28(5), 585–596.

Di Piazza, M.C., Pucci, M., Ragusa, A., and Vitale, G. (2010). A grid-connected system based on a real time pv emulator: Design and experimental set-up. In *IECON 2010 - 36th Annual Conference on IEEE Industrial Electronics Society*, 3237–3243.

Gonzalez-Llorente, J., Rambal-Vecino, A., Garcia-Rodriguez, L.A., Balda, J.C., and Ortiz-Rivera, E.I. (2016). Simple and efficient low power photovoltaic emulator for evaluation of power conditioning systems. In *2016 IEEE Applied Power Electronics Conference and Exposition (APEC)*, 3712–3716.

Hassan Hosseini, S.M. and Keymanesh, A.A. (2016). Design and construction of photovoltaic simulator based on dual-diode model. *Solar Energy*, 137, 594–607.

Hunter, G., Riedemann, J., Andrade, I., Blasco-Gimenez, R., and Peña, R. (2019). Power control of a grid-connected PV system during asymmetrical voltage faults. *Electrical Engineering*, 101(1), 239–250.

Ishaque, K., Salam, Z., and Taheri, H. (2011). Simple, fast and accurate two-diode model for photovoltaic modules. *Solar Energy Materials and Solar Cells*, 95(2), 586–594.

Khan, M.A., Haque, A., and Kurukuru, V.S.B. (2019). Intelligent control of a novel transformerless inverter topology for photovoltaic applications. *Electrical Engineering.*

Khouzam, K. and Hoffman, K. (1996). Real-time simulation of photovoltaic modules. *Solar Energy*, 56(6), 521–526.

Kim, Y., Lee, W., Pedram, M., and Chang, N. (2013). Dual-mode power regulator for photovoltaic module emulation. *Applied Energy*, 101, 730–739.

Mai, T.D., De Breucker, S., Baert, K., and Driesen, J. (2017). Reconfigurable emulator for photovoltaic modules under static partial shading conditions. *Solar Energy*, 141, 256–265.

Moussa, I. and Khedher, A. (2019). Photovoltaic emulator based on PV simulator RT implementation using XSG tools for an FPGA control: Theory and experimentation. *International Transactions on Electrical Energy Systems*, 29(8), e12024.

Moussa, I., Khedher, A., Bouallegue, A., Moussa, I., Khedher, A., and Bouallegue, A. (2019). Design of a Low-Cost PV Emulator Applied for PVECS. *Electronics*, 8(2), 232.

Muhsen, D.H., Ghazali, A.B., Khatib, T., and Abed, I.A. (2015). Parameters extraction of double diode photovoltaic module's model based on hybrid evolutionary algorithm. *Energy Conversion and Management*, 105, 552–561.

Mukerjee, A. and Dasgupta, N. (2007). DC power supply used as photovoltaic simulator for testing MPPT algorithms. *Renew. Energy*, 32(4), 587–592.

Nazar Ali, A., Premkumar, K., Vishnupriya, M., Manikandan, B.V., and Thamizhselvan, T. (2021). Design and development of realistic PV emulator adaptable to the maximum power point tracking algorithm and battery charging controller. *Sol. Energy*, 220, 473–490.

Piazza, M.C.D., Pucci, M., Ragusa, A., and Vitale, G. (2010). Analytical Versus Neural Real-Time Simulation of a Photovoltaic Generator Based on a DC–DC Converter. *IEEE Transactions on Industry Applications*, 46(6), 2501–2510.

Piazza, M.C.D. and Vitale, G. (2012). *Photovoltaic Sources: Modeling and Emulation.* Springer Science & Business Media. Google-Books-ID: X8DTKDfv06IC.

Ram, J.P., Manghani, H., Pillai, D.S., Babu, T.S., Miyatake, M., and Rajasekar, N. (2018). Analysis on solar PV emulators: A review. *Renew. Sustain. Energy Rev.*, 81, 149–160.

Razman, A. and Wei, T.C. (2017a). A comprehensive review on photovoltaic emulator. *Renew. Sustain. Energy Rev.*, 80, 430–452.

Razman, A. and Wei, T.C. (2017b). An adaptive controller for photovoltaic emulator using artificial neural network. *Indonesian Journal of Electrical Engineering and Computer Science*, 5(3), 556–563.

Razman, A. and Wei, T.C. (2017c). Improved control strategy for photovoltaic emulator using resistance comparison method and binary search method. *Solar Energy*, 153, 83–95.

Restrepo, C., Gonzalez-Castano, C., Munoz, J., Chub, A., Vidal-Idiarte, E., and Giral, R. (2021). An MPPT Algorithm for PV Systems Based on a Simplified Photo-Diode Model. *IEEE Access*, 9, 33189–33202.

Samara, S. and Natsheh, E. (2018). Modeling the output power of heterogeneous photovoltaic panels based on artificial neural networks using low cost microcontrollers. *Heliyon*, 4(11), e00972.

Sampaio, L.P. and Silva, S.A.O.d. (2017). Graphic computational platform integrated with an electronic emulator dedicated to photovoltaic systems teaching. *IET Power Electronics*, 10(14), 1982–1992.

Shuvho, M.B.A., Chowdhury, M.A., Ahmed, S., and Kashem, M.A. (2019). Prediction of solar irradiation and performance evaluation of grid connected solar 80kwp PV plant in Bangladesh. *Energy Reports*, 5, 714–722.

Sivaneasan, B., Yu, C.Y., and Goh, K.P. (2017). Solar Forecasting using ANN with Fuzzy Logic Preprocessing. *Energy Procedia*, 143, 727–732.

Tang, K.H., Chao, K.H., Chao, Y.W., and Chen, J.P. (2012). Design and Implementation of a Simulator for Photovoltaic Modules. *International Journal of Photoenergy.*

Ulaganathan, M. and Devaraj, D. (2016). Real coded genetic algorithm for optimal parameter estimation of solar photovoltaic model. In *2016 Int. Conf. Emerg. Trends Eng. Technol. Sci.*, 1–6. IEEE.

Ulaganathan, M. and Devaraj, D. (2019). Hardware and software co-emulation technique based solar photovoltaic sources emulator. In *2019 IEEE International Conference on Intelligent Techniques in Control, Optimization and Signal Processing (INCOS)*, 1–6.

Xenophontos, A., Rarey, J., Trombetta, A., and Bazzi, A.M. (2014). A flexible low-cost photovoltaic solar panel emulation platform. In *2014 Power and Energy Conference at Illinois (PECI)*, 1–6.

Yaïci, W., Longo, M., Entchev, E., and Foiadelli, F. (2017). Simulation Study on the Effect of Reduced Inputs of Artificial Neural Networks on the Predictive Performance of the Solar Energy System. *Sustainability*, 9(8), 1382.

Zagrouba, M., Sellami, A., Bouaïcha, M., and Ksouri, M. (2010). Identification of PV solar cells and modules parameters using the genetic algorithms: Application to maximum power extraction. *Solar Energy*, 84(5), 860–866.